



# Transverse Contraction-based Stability Analysis for Periodic Trajectories of Controlled Power Kites with Model Uncertainty

**Conference Paper****Author(s):**

Ahbe, Eva; [Wood, Tony A.](#) ; [Smith, Roy](#) 

**Publication date:**

2018

**Permanent link:**

<https://doi.org/10.3929/ethz-b-000327337>

**Rights / license:**

[In Copyright - Non-Commercial Use Permitted](#)

**Originally published in:**

<https://doi.org/10.1109/CDC.2018.8619106>

**Funding acknowledgement:**

642682 - Airborne Wind Energy System Modelling, Control and Optimisation (SBFI)

# Transverse Contraction-based Stability Analysis for Periodic Trajectories of Controlled Power Kites with Model Uncertainty

Eva Ahbe, Tony A. Wood, Roy S. Smith

**Abstract**—In this paper we propose a procedure for estimating the region in which a controller robustly stabilizes a system which is subject to affine parametric uncertainty by applying transverse contraction-based stability tools. The method consists of an optimization problem in which transverse contraction conditions are verified via sum-of-squares programs. The optimization approach can be used either to maximize the bounds on the allowable parameter uncertainty or to maximize the size of the region of contraction (ROC) given a fixed level of uncertainty. In a case study we apply the procedure to an Airborne Wind Energy system where the flight path of a power generating kite is controlled by a linear quadratic regulator based on a model which is prone to large parametric uncertainties. We consider periodic trajectories of the stabilized kite system and transform the dynamics into transversal coordinates for simplification of the controller design and reduction of the computational cost. The numerical results of the proposed optimization show that uncertainty in the steering gain parameter decreases the size of the ROC while uncertainty in wind speed or line length within the considered range of operating conditions does not affect the size of the robust ROC.

## I. INTRODUCTION

Airborne Wind Energy (AWE) denotes the research field around technologies aiming at extracting power from high-altitude winds with tethered aircrafts. The majority of concepts focus on energy generation via tethered rigid or flexible wing kites flying in crosswind conditions. For an overview of the field see [1]. One of the challenges the technology still faces lies in being able to guarantee a reliable operation of the system within a specified range of operating conditions. This particularly affects the development of the controllers enabling the autonomous operation of the kites. While there have been successfully tested control designs for kites in the past [2]–[5], the question of their reliability remains open.

Typically while generating power the motion pattern of the kite can be considered periodic, allowing for the application of limit cycle stability analysis tools. In a first approach, such tools were used in [6] to investigate guarantees for the stability of a path-tracking feedback control design for a kite flying periodic trajectories. Therein, the stabilizing region of a periodic path-stabilizing Linear Quadratic Regulator (LQR) was investigated via Lyapunov methods for a nominal

system model. However, in model-based approaches for the control of kites parametric uncertainty is usually significant as simplified models for complex interaction of kite, tether and actuator dynamics are used. Furthermore, the model parameters are typically hard to identify and/or slowly change over time [7].

The aim of this paper is to investigate how the stabilizing region of an LQR feedback design for path-tracking is affected by parametric uncertainty. As the uncertainty affects the location of the limit cycle Lyapunov tools are not applicable for this case and instead approaches based on contraction theory are employed.

Contraction methods analyze stability of nonlinear systems by considering the rate of change of an incremental distance between any two neighboring trajectories. If this distance is decreasing in a region of the state space then all trajectories in this region will eventually converge to a single trajectory. We further refer to this region as the region of contraction (ROC). Due to the periodic nature of the problem, we focus on transverse contraction introduced in [8]. Transverse contraction is a weaker form of contraction as it only analyses contraction in a transversal subspace of the systems.

In [9], a method for efficiently computing contraction metrics was introduced which employs methods based on sums-of-squares programs proposed in [10] for the efficient computational verification of polynomial positivity. This computational approach was extended in [11] and [12] to compute contraction metrics to verify local ROCs of systems with limit cycles. We apply this approach to a commonly used model for kite controller design, and extend it by both maximizing for larger estimates of ROCs as well as by considering parametric affine uncertainty in the system dynamics. For the latter we propose a verification algorithm where the uncertainty does not increase the number of indeterminants in the problem.

Further, we consider transverse contraction for the system in transverse coordinates. The transformation to transverse coordinates adds an initial computation cost, however, it offers several significant advantages. Firstly, the transformation to transverse coordinates reduces the systems dimension by one and reduces the number of the constraints, which both significantly decrease the computational costs of the numerical verification of the ROC. Secondly, the resulting feedback controller gains for the originally time-varying system will be static, i.e. associated to states and independent of time. Thirdly, the issue appearing in practice of selecting a suitable reference point on the trajectory is avoided, as there is a unique reference for the path-controller for any state

Eva Ahbe and Roy S. Smith are with the Automatic Control Laboratory, Swiss Federal Institute of Technology (ETH Zurich), Physikstrasse 3, 8092 Zurich, Switzerland, {ahbe, rsmith}@control.ee.ethz.ch.

Tony A. Wood is with the Department of Electrical and Electronic Engineering, University of Melbourne, wood.t@unimelb.edu.au

This work was supported by the Innovative Training Network (ITN) project funded by the European Union's Horizon 2020 research and innovation programme under the Marie Skłodowska-Curie Action (MSCA), grant agreement No. 642682.

inside the ROC, for which we propose a recovering strategy.

#### A. Notation

We use  $\mathbb{R}[x]$  to denote polynomials with real coefficients in the indeterminants  $[x_1, \dots, x_n]$ . A polynomial is a sum-of-squares (SOS) if it can be written as  $p(x) = \sum_i q_i^2$ ,  $q_i \in \mathbb{R}[x]$  and the set of all SOS polynomials is indicated by  $\Sigma[x]$ . A symmetric matrix with polynomial entries  $F(x) \in \mathbb{R}[x]^{n \times n}$  is a SOS matrix if for a vector of indeterminants  $y = [y_1, \dots, y_n]^T$  the scalar polynomial  $y^T F(x) y$  is SOS in  $\mathbb{R}[x, y]$ . The set of SOS matrices is denoted by  $\Sigma[x]^{n \times n}$ .

### II. TRANSVERSE CONTRACTION

We consider autonomous nonlinear systems,

$$\dot{x} = f(x), \quad (1)$$

with state  $x(t) \in \mathbb{R}^n$ , initial state  $x(0) = x_0$  and the solution denoted by  $\phi(x_0, t)$  for  $t > 0$ . In particular, we are interested in systems whose solutions exhibit periodic behavior. We call a solution  $\tilde{x}(t) = \phi(\tilde{x}_0, t)$  of the system (1) a periodic orbit if  $\tilde{x}(0) = \tilde{x}(T)$  with a minimum period  $T > 0$  and denote all points on the orbit by  $\Gamma = \{x \in \mathbb{R}^n | x = \tilde{x}(t), t \in [0, T]\}$ .

#### A. Transverse Contraction Criteria

The aim of this paper is to obtain estimates of the region of stability for an autonomous system with a stable limit cycle. We hereby define stability of a region in the sense of a region in which the system is *transverse contracting*, a concept derived from Zhukovsky stability [13]. We follow the definition of transverse contraction as presented in, e.g., [11] and [14]. Throughout this paper we consider a Riemannian distance metric function of the form  $V(x, \delta_x) = \delta_x^T M(x) \delta_x$ , where  $\delta_x$  denotes a virtual displacement, i.e. a linear tangent differential form representing an incremental displacement of  $x(t)$  at a fixed time. Further,  $M(x)$  is a Riemannian metric, thus positive-definite for all  $x$ . Transverse contraction can then be defined by the following theorem (as in [11]).

**Theorem 1:** Consider the system (1) on a subset  $K \subset \mathbb{R}^n$ . Let  $K$  be compact, smoothly path-connected, and strictly forward invariant. If there exists a metric function  $V(x, \delta_x)$  satisfying

$$\frac{\partial V}{\partial x} f(x) + \frac{\partial V}{\partial \delta_x} \frac{\partial f}{\partial x} \delta_x \leq -\lambda V(x, \delta_x) \quad (2)$$

for all  $\delta_x \neq 0$  such that the orthogonality condition  $\frac{\partial V}{\partial \delta_x} f(x) = 0$  is satisfied, then the system (1) is called *transverse contracting* in  $K$ . For every two solutions  $x_1$  and  $x_2$  with initial conditions in  $K$  there then exists a time reparametrizations  $\nu(t)$  such that  $x_1(t) \rightarrow x_2(\nu(t))$  as  $t \rightarrow \infty$ . Further, any solution starting in  $x(0) \in K$  converges to  $\tilde{x}(t)$ , the unique limit cycle of the system, as  $t \rightarrow \infty$ .

A proof of this theorem can be found in [11]. We call a region  $K \in \mathbb{R}^n$  in which the transverse contraction criteria stated in the theorem are satisfied an ROC and the corresponding metric  $M$  a contraction metric. For  $V(x, \delta_x) = \delta_x^T M(x) \delta_x$  the orthogonality condition becomes  $\delta_x^T M f(x) = 0$ .

#### B. Contraction in the Transverse Subspace

In order to obtain an estimate of the ROC of the system given in (1) we can employ SOS relaxations of polynomial positivity problems, as in [11], [12], [15], for finding contraction metrics. The computational cost thereby strongly depends on the state dimension. It is thus favorable to reduce the state dimension which is made possible by exploiting the orthogonality condition. We then obtain a  $(n-1)$ -dimensional subspace defined by all  $\delta_x$  satisfying the orthogonality condition, i.e., the subspace defined by the hyperplanes orthogonal to the system flow. We call this subspace the *transverse subspace* for which we obtain the associated system dynamics by a transformation of the system into transverse coordinates. This transformation was introduced in [16] and [17] and employed for stability analysis of limit cycles in [18], and [6]. We briefly restate the transformation law for completeness. For derivations see [16] and [18].

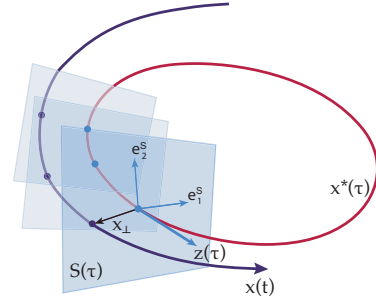


Fig. 1. Illustration of the transversal coordinates. The hyperplanes  $S(\tau)$  are defined by a  $(n-1)$ -dimensional coordinate system  $\{e_i^S\}_{i=1}^{n-1}$ . The vector  $z(\tau)$  is normal to the hyperplane  $S(\tau)$ .

Transversal coordinates are obtained from a smooth and locally well-defined transformation of any  $x \in \mathbb{R}^n$  in a sufficiently close neighborhood of the orbit  $\Gamma$  into a pair of coordinates  $(\tau, x_\perp) \in S \times \mathbb{R}^{n-1}$ . For every  $t \in [0, T]$  we can then define an  $(n-1)$ -dimensional periodic time-varying hyperplane  $S$  with  $S(0) = S(T)$  which is transversal to  $\Gamma$  at  $\tilde{x}(t)$ , i.e.,  $f(\tilde{x}(t)) \notin S(t)$ . Given any  $x$  in a sufficiently close neighborhood of  $\tilde{x}(t)$ ,  $\tau$  specifies the corresponding transversal hyperplane and  $x_\perp$  is the position on that hyperplane such that  $x_\perp = 0 \Leftrightarrow x = \tilde{x}(\tau)$ . For a visualization see Fig. 1. The transversal hyperplanes  $S(\tau)$  are defined by

$$S(\tau) = \{x \in \mathbb{R}^n | z(\tau)^T (x - \tilde{x}(\tau)) = 0\}, \quad (3)$$

where  $z(\tau) : [0, T] \rightarrow \mathbb{R}^n$  is a smooth, periodic vector function chosen to lie tangential to the system flow, i.e.  $z(\tau) = \frac{f(\tilde{x}(\tau))}{\|f(\tilde{x}(\tau))\|_2}$ . With this, a projection operator  $\Pi(\tau)$  can be constructed that maps any point  $x$  in the neighborhood of  $\Gamma$  into its transversal coordinates on the respective hyperplane,  $x_\perp = \Pi(\tau) (x - \tilde{x}(\tau))$ . The dynamics in transversal coordinates then follow as

$$\dot{x}_\perp = \left[ \frac{d}{d\tau} \Pi(\tau) \right] \dot{\tau} \Pi(\tau)^T x_\perp + \Pi(\tau) f(\tilde{x}(\tau)) + \Pi(\tau)^T x_\perp, \quad (4)$$

$$\dot{\tau} = \frac{z^T f(\tilde{x}(\tau)) + \Pi(\tau)^T x_\perp}{z(\tau)^T f(\tilde{x}(\tau)) - \frac{\partial z(\tau)}{\partial \tau}^T \Pi(\tau)^T x_\perp}. \quad (5)$$

In order for the dynamics of  $\tau$  to be well-defined the denominator of (5) has to be non-zero and is thus positive,

$$d(x_\perp, \tau) := z(\tau)^T f(\tilde{x}(\tau)) - \frac{\partial z(\tau)^T}{\partial \tau} \Pi(\tau)^T x_\perp > 0. \quad (6)$$

We now consider the transverse differential coordinates  $(\delta_\tau, \delta_\perp)$ , i.e. virtual displacements in  $\tau$  and  $x_\perp$ . Let

$$\begin{bmatrix} \delta_\tau \\ \delta_\perp \end{bmatrix} = \Theta(x, t) \delta_x, \quad (7)$$

where  $\Theta$  is the transformation to transverse differential coordinates obtained from the Jacobian of  $\Pi$ . By construction,  $\delta_\perp$  lies in the subspace defined by all  $\delta_x$  for which we can find a Riemannian metric  $M^\dagger(x)$  such that  $\delta_x^T M^\dagger(x) f(x) = 0$ .

We now aim to find a  $M^\dagger(x)$  which is also a contraction metric for the transversal system. To this end, consider the time derivative of the differential forms ([11], [17])

$$\frac{d}{dt} \begin{bmatrix} \delta_\tau \\ \delta_\perp \end{bmatrix} = \begin{bmatrix} 0 & * \\ 0 & A_\perp(x) \end{bmatrix} \begin{bmatrix} \delta_\tau \\ \delta_\perp \end{bmatrix}, \quad (8)$$

where  $A_\perp(x)$  is the Jacobian of the transverse dynamics in (4), defined as

$$A_\perp = \frac{\partial f_\perp(x)}{\partial x_\perp} = \left[ \frac{d}{dt} \Pi(\tau) \right] \Pi(\tau)^T + \Pi(\tau) \frac{\partial f(x)}{\partial x} \Pi(\tau)^T, \quad (9)$$

where  $f_\perp(x) = \dot{x}_\perp$ . Following Lyapunov stability arguments, the differential system (8) is stable if there exists a positive symmetric matrix  $M_\perp \in \mathbb{R}^{n-1 \times n-1}$  satisfying

$$A_\perp^T(x) M_\perp(x) + M_\perp(x) A_\perp(x) + \dot{M}_\perp(x) < -\beta I \quad (10)$$

for some  $0 < \beta$  and for all  $x \in K$ . Here,

$$\dot{M}_{\perp ij}(x) = \frac{\partial M_{\perp ij}}{\partial x_\perp} f_\perp(x) + \frac{\partial M_{\perp ij}}{\partial \tau} \dot{\tau}, \quad (11)$$

where  $i, j$  denote the row and column of the matrix  $M_\perp$ .

Let  $x_p = [\tau, x_\perp]^T$  and  $\delta_p = [\delta_\tau, \delta_\perp]^T$ , then with the metric found in (10) we can define a distance function metric

$$V(x_p, \delta_p) = \delta_p^T M(x_p) \delta_p. \quad (12)$$

Imposing  $\delta_\tau M(x_p) \delta_\perp = 0$  and dropping the  $x_p$  notation we get

$$V(x_p, \delta_p) = \begin{bmatrix} \delta_\tau \\ \delta_\perp \end{bmatrix}^T \begin{bmatrix} M_\tau & 0 \\ 0 & M_\perp \end{bmatrix} \begin{bmatrix} \delta_\tau \\ \delta_\perp \end{bmatrix} = \delta_\tau^2 + \delta_\perp^T M_\perp \delta_\perp, \quad (13)$$

where we assume w.l.o.g  $M_\tau = 1$ . This metric satisfies the transverse contraction criteria stated in Theorem 1 and represents thus the desired contraction metric  $M^\dagger$ .

### III. AFFINE PARAMETRIC UNCERTAINTY

We now consider dynamical systems in polynomial form with additive parametric uncertainty

$$\dot{x} = f^\psi(x) = f(x) + \psi(x), \quad (14)$$

where  $f, \psi : \mathbb{R}^n \rightarrow \mathbb{R}[x]^n$ ,  $f(x)$  are the known nominal dynamics and  $\psi \in \mathcal{D}_\sigma$  with  $\mathcal{D}_\sigma := \{\psi : \psi(x) = \sigma \Psi(x) \ \forall x \in \mathbb{R}^n, \ \underline{\sigma} \leq \sigma \leq \bar{\sigma}\}$ . Here,  $\underline{\sigma}, \sigma, \bar{\sigma} \in \mathbb{R}^n$ ,  $\underline{\sigma}, \bar{\sigma}$  denote the lower and upper bound of the parametric uncertainty  $\sigma$ , and  $\Psi(x) \in \mathbb{R}[x]^{n \times n}$  is known. Note that we allow for the uncertainty to change the location of the equilibrium state

of (14). We define  $A_\perp^\psi(x) := \frac{\partial f_\perp^\psi(x)}{\partial x} = \frac{\partial (f(x) + \psi(x))_\perp}{\partial x}$ . The condition of (10) for the contracting region of (14) is then

$$A_\perp^\psi(x)^T M_\perp(x) + M_\perp(x) A_\perp^\psi(x) + \dot{M}_\perp^\psi(x) < -\beta I, \quad (15)$$

for some  $\beta > 0$ , for all  $x \in K$  and all  $\psi \in \mathcal{D}_\sigma$ . In (15)  $\dot{M}_\perp^\psi(x)$  comes from replacing  $f_\perp(x)$  with  $f_\perp^\psi(x)$  in (11). Note that condition (15) represents sufficient conditions for the stability of (14). Therefore, in general, the metric  $M_\perp(x)$  can also be dependent on  $\sigma$ . In numerical implementations this leads to potentially less conservative results at the exchange of (significantly) increased computational costs.

Since  $\mathcal{D}_\sigma$  has infinitely many elements, for each  $x \in K$  condition (15) poses infinitely many constraints. We define

$$\mathcal{Z} := \{\psi : \psi(x) = \sigma \Psi(x), \text{ with } \sigma_i \in \{\underline{\sigma}_i, \bar{\sigma}_i\}, \forall i\} \quad (16)$$

where  $\mathcal{Z}$  is a finite subset of  $\mathcal{D}_\sigma$ . Thus containing only a finite number of elements,  $\mathcal{Z}$  can now be used to express (15) as a finite number of constraints in  $\sigma$ . The outline of the following Proposition is similar to [19].

*Proposition 1:* If

$$A_\perp^\zeta(x)^T M_\perp(x) + M_\perp(x) A_\perp^\zeta(x) + \dot{M}_\perp^\zeta(x) < -\beta I \quad (17)$$

holds with  $\beta > 0$  for all  $x \in K$  and for all  $\zeta \in \mathcal{Z}$ , then (15) holds for all  $\psi \in \mathcal{D}_\sigma$ .

The proof is similar to [19] and omitted for brevity.

### IV. ALGORITHM FOR COMPUTING THE ROBUST ROC

We present an algorithm to efficiently compute an estimate of the ROC for polynomial systems with limit cycles. Similar to the computational approach in [6] we employ a numerical method proposed in [10], in which semidefinite relaxations of the Positivstellensatz [20] are used to formulate SOS-programs to test polynomial positivity as semidefinite program efficiently. Non-polynomial systems can be considered by a Taylor series approximation.

#### A. Nominal ROC

We first present the algorithm to test for a region  $\hat{\mathcal{B}} = \{x_\perp : x_\perp^T M_\perp(x_\perp, \tau) x_\perp \leq \hat{\rho}\}$  to be an ROC of the nominal dynamics, i.e., assuming zero uncertainty,  $\sigma = 0$  in (14). Defined as such, this region represents a ball centered around the reference trajectory and includes all points whose distance to the reference trajectory with respect to the metric  $M_\perp$  is less than the radius  $\hat{\rho}$ .

A region  $\hat{\mathcal{B}}$  is an ROC of a nominal system if it satisfies condition (10). We define  $\hat{C} := A_\perp^T(x_\perp, \tau) M_\perp(x_\perp, \tau) + M_\perp(x_\perp, \tau) A_\perp(x_\perp, \tau) + \dot{M}_\perp(x_\perp, \tau)$ . Additionally, we obtain a constraint for the ROC from condition (6), as we require the transformation to transversal coordinates to be well-defined. Note that the term  $d(x_\perp, \tau)$  in (6) also appears in the denominator of  $\dot{M}_\perp(x_\perp, \tau)$ . However, since (6) is constraint to be positive  $\hat{C}$  can be multiplied by it without changing the outcome of condition (10), such that all terms result in the required polynomial form.

We aim at enlarging the estimate of the ROC  $\hat{\mathcal{B}}$  by optimizing over the metric  $M_\perp$  satisfying these two conditions. We fix the radius  $\hat{\rho}$  of  $\hat{\mathcal{B}}$  to a positive constant as an optimization

over both  $\hat{\rho}$  and  $M_\perp$  would not lead to larger ROCs but to a mere rescaling of the coefficients of  $M_\perp$ . In order to still have a measure to increase the ROC we need to include an additional constraint in which we are optimizing over the radius of a ball  $\mathcal{B}_2 = \{x_\perp : x_\perp^T x_\perp \leq \rho_2\}$  such that  $\mathcal{B}_2 \subset \hat{\mathcal{B}}$ , similar to an approach employed in [6]. This encourages the algorithm to find metrics which increase the size of the ROC during the optimization over  $M_\perp$ . The optimization problem is expressed as follows.

$$\max_{M_\perp, s_1, s_2, s_3} \quad \rho_2 \quad (18a)$$

$$\text{subject to} \quad M_\perp(x_\perp, \tau) \in \Sigma[x_\perp, \tau]^{n-1 \times n-1}, \quad (18b)$$

$$-\hat{C}(x_\perp, \tau) - (\hat{\rho} - \hat{\mathcal{B}})s_1(x_\perp, \tau) \in \Sigma[x_\perp, \tau]^{n-1 \times n-1}, \quad (18c)$$

$$d(x_\perp, \tau) - (\hat{\rho} - \hat{\mathcal{B}})s_2(x_\perp, \tau) \in \Sigma[x_\perp, \tau], \quad (18d)$$

$$-(\rho_2 - \mathcal{B}_2)s_3(x_\perp, \tau) + (\hat{\rho} - \hat{\mathcal{B}}) \in \Sigma[x_\perp, \tau], \quad (18e)$$

$$s_1(x_\perp, \tau) \in \Sigma[x_\perp, \tau]^{n-1 \times n-1}, \quad (18f)$$

$$s_2(x_\perp, \tau), s_3(x_\perp, \tau) \in \Sigma[x_\perp, \tau]. \quad (18g)$$

The multipliers  $s_1$ ,  $s_2$  and  $s_3$  result from the application of the Positivstellensatz and are constrained to be SOS polynomials and SOS matrices, respectively. All multipliers as well as the metric  $M_\perp$  are variables used to test sufficient conditions and can thus be chosen to be of any (even) polynomial degree. Choosing larger degrees can potentially lead to larger verified ROC, however the computational costs increase polynomially. To demonstrate the structure of  $M_\perp$  let  $n = 3$  and  $m$  be the degree of  $M_\perp$ , then

$$M_\perp(x_\perp, \tau) = \begin{bmatrix} \sum_{i,j} a_{ij}(\tau) x_{\perp 1}^i x_{\perp 2}^j & \sum_{i,j} b_{ij}(\tau) x_{\perp 1}^i x_{\perp 2}^j \\ \sum_{i,j} b_{ij}(\tau) x_{\perp 1}^i x_{\perp 2}^j & \sum_{i,j} d_{ij}(\tau) x_{\perp 1}^i x_{\perp 2}^j \end{bmatrix}.$$

The algorithm (18) is bilinear in the coefficients of the multipliers and the metric  $M_\perp$ . As proposed in, e.g. [19], [21] and others, this can efficiently, although potentially suboptimally, be solved by fixing either one of the variables while optimizing over the other. This turns the bilinear problem into two convex problems solved alternatingly in two steps. For the initialization of the alternation we use the (zero degree) metric resulting from solving (10) as a periodic Lyapunov equation [17]. For this initial metric we then need sufficiently small radii  $\rho_2$  and  $\hat{\rho}$  for the first step to be feasible, which we can find by bisection.

The algorithm (18) is dependent on the time-parametrization  $\tau$ . We efficiently treat this dependency in a similar way as employed in [6] by solving the optimization (18) for  $N$  fixed and equally spaced values of  $\tau$  over the whole period. For the metric  $M_\perp$  we can translate this discretization of  $\tau$  by casting the entries of  $M_\perp$  as piecewise linear in  $\tau$  as described in [6].

## B. Robust ROC

We are now interested in searching for ROCs in the presence of additive parametric uncertainty, referred to as robust ROCs. A general uncertainty structure would introduce a set constraint on an additional indeterminant. This would result in an increased dimension of the problem as well as

additional multipliers in the algorithm (18), and a significant increase of computational costs. However, when considering affine uncertainty in the dynamics, the results of Proposition 1 can be used to allow for the uncertainty to enter the problem without increasing the number of indeterminants and thereby the complexity of the problem.

Algorithm (18) can now be extended to estimate the robust ROC of an uncertain system. Hereby we can either set a fixed uncertainty level and then optimize for the largest ROC given this choice. An other possibility is to prescribe a fixed region and then maximize the uncertainty for which this region is a ROC. Since in general maximizing the size of ROC and the magnitude of uncertainty at the same time represents a trade-off, i.e. the larger the ROC the smaller the maximum uncertainty and vice versa, we are not considering an optimization over both at the same time.

In order to formulate an optimization similar to (18) for estimating robust ROC an adjustment of constraint (18c) is required such that it now tests for condition (17). Let  $\hat{C}_\zeta = A_\perp^\zeta(x)^T M_\perp(x) + M_\perp(x) A_\perp^\zeta(x) + \dot{M}_\perp^\zeta(x)$  for an element  $\zeta \in \mathcal{Z}$ , then for each  $\zeta \in \mathcal{Z}$  we obtain a condition

$$-\hat{C}_\zeta(x_\perp, \tau) - (\hat{\rho} - \hat{\mathcal{B}})s_\zeta(x_\perp, \tau) \in \Sigma[x_\perp, \tau]^{n-1 \times n-1} \quad (19)$$

with  $s_\zeta \in \Sigma[x_\perp, \tau]^{n-1 \times n-1}$  being the associated multiplier.

A procedure for estimating the robust ROC then follows from iterating over the following steps.

### Step 1: Finding multipliers

$$\begin{aligned} &\text{find:} && s_\zeta, s_2, s_3 \\ &\text{subject to} && (19), (18d), (18e), (18f), (18g) \\ &\text{with fixed} && M_\perp, \rho_2, \tilde{\sigma} \end{aligned}$$

### Step 2 - Choice 1: Maximizing robust ROC

$$\begin{aligned} &\max_{\rho_2, M_\perp} && \rho_2 \\ &\text{subject to} && (19), (18b), (18d), (18e) \\ &\text{with fixed} && s_\zeta, s_2, s_3, \tilde{\sigma} \end{aligned}$$

### Step 2 - Choice 2: Maximizing uncertainty bounds

$$\begin{aligned} &\max_{\tilde{\sigma}, M_\perp} && \tilde{\sigma} \\ &\text{subject to} && (19), (18b)^1, (18d)^1, (18e)^1 \\ &\text{with fixed} && s_\zeta, s_2, s_3, \rho_2, M_\perp^1 \end{aligned}$$

where  $\tilde{\sigma} = \{\underline{\sigma}, \bar{\sigma}\}$ . With this algorithm either a maximum estimate for the size of ROC for a fixed amount of uncertainty can be obtained from alternating between Step 1 and Choice 1, or a maximum amount of uncertainty for a fixed minimum size of ROC can be obtained by alternating over Step 1 and Choice 2. The results from (18) can hereby be used for initialization.

<sup>1</sup>Note that in Choice 2, optimizing over  $M_\perp$  is optional; it can lead to larger estimates however  $M_\perp$  and  $\tilde{\sigma}$  then appear bilinearly such that a subiteration leading to an additional iteration step is required. Thereby,  $\tilde{\sigma}$  is first maximized for a fixed  $M_\perp$  and then a feasibility problem is solved for  $M_\perp$  with fixed  $\tilde{\sigma}$ .

## V. CASE STUDY: KITE MODEL WITH UNCERTAINTY

We apply the computation of robust ROCs to a numerical case study of an autonomous kite system that is feedback-stabilized in order to follow a desired trajectory.

### A. Kite Dynamics and Reference Trajectory

The kite dynamics are described as a first order kinematic model of the states  $x = (\theta, \phi, \gamma)$ , where  $\theta$  denotes the elevation angle,  $\phi$  the azimuth angle, and  $\gamma$  the orientation angle of the kite ( $\gamma = 0$  when pointing towards the Zenith),

$$\dot{\theta} = \frac{v_k}{L} \cos(\gamma), \quad (23a)$$

$$\dot{\phi} = \frac{v_k}{L} \cos(\theta)^{-1} \sin(\gamma), \quad (23b)$$

$$\dot{\gamma} = v_k G u, \quad (23c)$$

where  $v_k = v_w E \cos(\theta) \cos(\phi)$ ,  $E = C_L/C_D$  is the glide ratio with  $C_L$  denoting the lift coefficient and  $C_D$  the drag coefficient.  $L$  is the line length,  $v_w$  is the wind speed,  $G$  is the steering gain and  $u$  is the input. This model is similar to the models employed for guidance control design in [3], [7].

We consider an additive uncertainty for the following parameters:

- 1) Uncertainty in wind speed:  $v_w = v_{w0} + \sigma_{v_w}$
- 2) Uncertainty in steering gain:  $G = G_0 + \sigma_G$
- 3) Uncertainty in line length:  $L = L_0 + \sigma_L$

Here,  $v_{w0}, G_0, L_0$  denote the nominal values and  $\sigma_{v_w}, \sigma_G, \sigma_L$  the respective uncertainties.

Desired periodic trajectories for the kite system to follow are obtained from an optimization problem which is solved with ACADO [22]. Therein, the tether force  $F(x(t), u(t))$  in an aerodynamic equilibrium is maximized over one period  $T$ ,

$$\begin{aligned} \max_{x(\cdot), u(\cdot), x_0, T} \quad & \frac{1}{T} \int_0^T F(x(t), u(t)) dt \quad (24) \\ \text{subject to} \quad & \dot{x} = f(x(t), u(t)) \\ \forall t \in [0, T] \quad & \underline{c} \leq x(t) \leq \bar{c} \\ & \underline{b} \leq u(t) \leq \bar{b} \\ & x(0) = x(T) = x_0 \end{aligned}$$

where  $f(x(t), u(t))$  are the dynamics (23a). The state constraints  $(\underline{c}, \bar{c}) \in \mathbb{R}^3$  ensure that the kite stays in crosswind flight conditions, prevent looping and enforce figure-eight trajectories in an upward direction. The input constraints  $(\underline{b}, \bar{b}) \in \mathbb{R}$  restrict the turning rate to comply with physical limits. By solving (24) we obtain the trajectory  $x^*(t)$  and open-loop inputs  $u^*(t)$  of a desired reference orbit  $\Gamma^*$ .

### B. Feedback Controller Implementation

We can now compute feedback-stabilizing gains for the system (23a) to follow the reference trajectory  $\Gamma^*$ . For the controller design we use gains obtained from solving a periodic time-varying Riccati equation for a Linear Quadratic Regulator. For this we first linearize the transverse dynamics of (23a) around  $\Gamma^*$  such that they appear in the form  $\dot{x}_\perp \approx A_\perp(\tau)x_\perp + B_\perp(\tau)u_\perp$ , where  $u_\perp = K_{LQR}(\tau)x_\perp$

is the transverse component of the input resulting from the feedback control,  $A_\perp(\tau)$  is the transverse Jacobian (9) evaluated around  $\Gamma^*$  and  $B_\perp(\tau)$  is obtained from  $B_\perp(\tau) = \Pi(\tau) \frac{\partial f(\bar{x}(\tau), \bar{u}(\tau))}{\partial u}$ . Note, that by using this approach we obtain a feedback-law which is independent of time and only depends on the location of the kite with respect to  $S(\tau)$ .

### C. Finding the Hyperplane Corresponding to a Given $x$

For any given value of  $\tau$ , the corresponding hyperplane and coordinates of any state  $x$  on that hyperplane can be analytically computed by the equations in Section II-B. However, in practice, when we want to apply the feedback gains computed from transversal coordinates we need to be able to reverse this mapping, i.e. given a state  $x$  of the system, we need to know which hyperplane it corresponds to. Since the control gains are parametrized by  $\tau$  the information of the corresponding hyperplane to a given state  $x$  is crucial and can be obtained numerically. Let

$$T_\tau := \{\tau \in [0, T] : z(\tau)^T(x - \tilde{x}(\tau)) = 0\} \quad (25)$$

be the set containing all  $\tau$  for which the given  $x$  lies on the  $S(\tau)$  as by condition (3). For each  $\tau \in T_\tau$  the state can then be transformed into transversal coordinates  $x_\perp$  via the corresponding projection operator  $\Pi(\tau)$ . From solving the ROC algorithm offline, we have the information of the size of the ROC and the corresponding metric. For each pair  $(\tau, x_\perp)$  obtained from  $T_\tau$  the condition

$$x_\perp^T M_\perp(x_\perp, \tau) x_\perp < \hat{\rho} \quad (26)$$

can then be checked. If the given state  $x$  is inside the ROC, condition (26) will return a unique pair  $(\tau, x_\perp)$  satisfying it. The uniqueness is hereby guaranteed by condition (18d), which can thus be understood as a non-intersecting constraint for the ROC on the hyperplanes. If the state is outside of the well-defined region then there is no uniquely corresponding hyperplane and thus no guaranteed unique stabilizing gain. For this case a control strategy could, e.g., consist in a set of desirable trajectories with their respective ROCs covering the state space, similar to an idea proposed in [23].

### D. Results

We compute estimates of the robust ROCs for the feedback-stabilized transverse kite dynamics with nominal parameter values:  $v_{w0} = 6$  m/s,  $G_0 = 1.25$ ,  $L_0 = 60$  m.

The closed loop system is approximated by a third order Taylor series around the reference trajectory. We estimate the robust ROC for each of the three cases of uncertainty listed in Section V-A, where we applied Choice 1 for the uncertainty in the steering gain and Choice 2 for the uncertainty in wind speed. For the uncertainty in the line length both Choice 1 and Choice 2 were tested.

We choose  $N = 50$  discrete values for  $\tau$  over the period  $T$ . In both the nominal and robust implementation we limit the degree of the metrics to 2, of the multipliers  $s_1$  and  $s_\zeta$  to 6, and of multipliers  $s_2$  and  $s_3$  to 2. Note that since sufficient conditions are tested any results shown here



represent lower bounds on the true robust ROC and true maximum uncertainty.

The verification algorithms are implemented using the SOS-module of YALMIP [24] and the resulting semidefinite programs were solved with MOSEK version 8.0.

Fig. 2 presents the nominal ROC as well as the robust ROCs obtained for uncertainty levels of  $\pm 20\%$  and  $\pm 40\%$  in the steering gain. As the figure illustrates, the verified robust ROC of the system shrinks with increasing uncertainty. Fig. 3 shows a rotated view of the ROC for the nominal case.

For uncertainty in wind speed the minimum size of the robust ROC was fixed to  $\rho_2 = 0.75 \cdot \rho_2^{\text{nom}}$ , where  $\rho_2^{\text{nom}}$  is the maximum radius obtained from the nominal calculations (18). The maximum for the lower and upper uncertainty returned by the optimization via Choice 2 hits the limits of typical operating conditions of 4-10 m/s which were set as stopping criteria of the algorithm. Simulations of the dynamics show that uncertainty in the wind speed in this range does not affect the location of the trajectories of the system but only affects how fast they evolve.

We obtain a similar result for the uncertainty in line length as for the wind speed when computing the maximum uncertainty by Choice 2. Here, the operating condition was set to 40-100 m and both limits were reached by the optimization. The results from Choice 1, where the robust ROC was maximized for a fixed uncertainty in line length confirms this result: for each fixed uncertainty level the stopping criterion consisting of the size of the nominal ROA was reached. Simulations of the system with uncertainty in line length show that, in contrary to the case of uncertainty in wind speed, for this case the trajectories including the location of the limit cycle are affected.

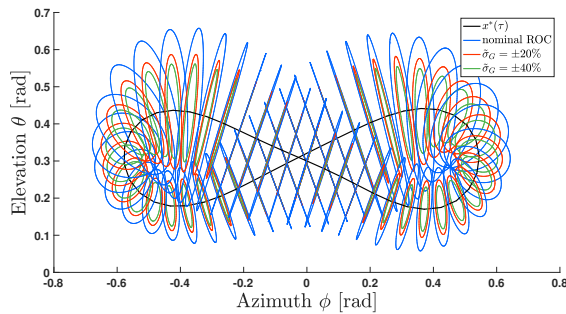


Fig. 2. The nominal ROC (blue lines) and the robust ROC for an uncertainty level of  $\pm 20\%$  (red lines) and of  $\pm 40\%$  (green lines) in the steering gain are shown on each hyperplane  $S(\tau)$ .

## REFERENCES

- [1] U. Ahrens, M. Diehl, and R. Schmehl, *Airborne Wind Energy*. Heidelberg, Germany: Springer, 2013.
- [2] L. Fagiano, A. U. Zraggen, M. Morari, and M. Khammash, "Automatic crosswind flight of tethered wings for airborne wind energy: modeling, control design and experimental results," *IEEE Trans. Control Syst. Technol.*, vol. 22, no. 4, pp. 1433–1447, 2014.
- [3] M. Erhard and H. Strauch, "Flight control of tethered kites in autonomous pumping cycles for airborne wind energy," *Control Eng. Pract.*, vol. 40, pp. 13–26, 2015.
- [4] N. Rontsis, S. Costello, I. Lymperopoulos, and C. N. Jones, "Improved path following for kites with input delay compensation," in *IEEE Conf. Decis. Control*. IEEE, 2015, pp. 656–663.

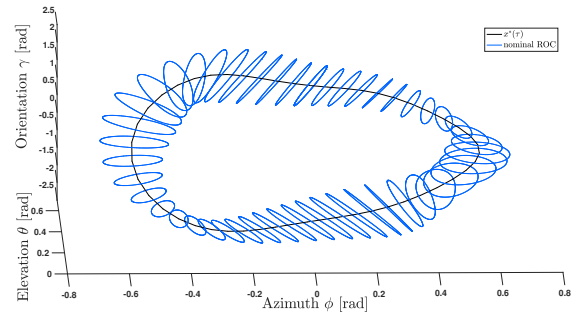


Fig. 3. A rotated 3D view of the nominal ROC displayed in Fig. 2. The  $\gamma$ -axis is scaled for illustration purposes.

- [5] T. A. Wood, H. Hesse, and R. S. Smith, "Predictive Control of Autonomous Kites in Tow Test Experiments," *IEEE Control Syst. Lett.*, vol. 1, no. 1, pp. 110–115, 2017.
- [6] E. Ahbe, T. A. Wood, and R. S. Smith, "Stability Verification for Periodic Trajectories of Autonomous Kite Power Systems," in *Proc. Eur. Control Conf.*, Limassol, Cyprus, 2018.
- [7] T. A. Wood, H. Hesse, A. U. Zraggen, and R. S. Smith, "Model-based flight path planning and tracking for tethered wings," in *Proc. IEEE Conf. Decis. Control*, 2015, pp. 6712–6717.
- [8] G. Borg, *A Condition for the Existence of Orbitally Stable Solutions of Dynamical Systems*. Stockholm. Handl. 153: Kungl. Tekn. Hogskol., 1960.
- [9] E. M. Aylward, P. A. Parrilo, and J.-J. E. Slotine, "Stability and robustness analysis of nonlinear systems via contraction metrics and SOS programming," *Automatica*, vol. 44, pp. 2163–2170, 2008.
- [10] P. A. Parrilo, "Structured Semidefinite Programs and Semialgebraic Geometry Methods in Robustness and Optimization," Ph.D. dissertation, California Institute of Technology, 2000.
- [11] I. R. Manchester and J.-J. E. Slotine, "Transverse contraction criteria for existence, stability, and robustness of a limit cycle," *Syst. Control Lett.*, vol. 63, pp. 32–38, 2014.
- [12] J. Z. Tang and I. R. Manchester, "Transverse contraction criteria for stability of nonlinear hybrid limit cycles," in *53rd IEEE Conf. Decis. Control*. IEEE, dec 2014, pp. 31–36.
- [13] G. Leonov, "Strange Attractors and Classical Stability Theory," *Nonlinear Dyn. Syst. theory*, vol. 8, no. 1, pp. 49–96, 2008.
- [14] P. Giesl and S. Hafstein, "Construction of a CPA contraction metric for periodic orbits using semidefinite optimization," *Nonlinear Anal.*, vol. 86, pp. 114–134, 2013.
- [15] J. Z. Tang, "Optimization-based Framework for Stability and Robustness of Bipedal Walking Robots," Ph.D. dissertation, Univ. of Sydney, 2017.
- [16] J. K. Hale, *Ordinary Differential Equations*. R.E. Krieger Pub. Co., New York, 1980.
- [17] J. Hauser and C. C. Chung, "Converse Lyapunov functions for exponentially stable periodic orbits," *Syst. Control Lett.*, vol. 23, pp. 27–34, 1994.
- [18] I. R. Manchester, "Transverse Dynamics and Regions of Stability for Nonlinear Hybrid Limit Cycles," in *IFAC Proc. Vol.*, vol. 44, no. 1. IFAC, 2011, pp. 6285–6290.
- [19] U. Topcu and A. Packard, "Local Stability Analysis for Uncertain Nonlinear Systems," *IEEE Trans. Automat. Contr.*, vol. 54, no. 5, pp. 1042–1047, 2009.
- [20] G. Stengle, "A Nullstellensatz and a Positivstellensatz in Semialgebraic Geometry," *Math. Ann.*, vol. 207, pp. 87–97, 1974.
- [21] Z. Jarvis-Wloszek, R. Feeley, W. Tan, K. Sun, and A. Packard, "Controls Applications of Sum of Squares Programming," in *Posit. Polynomials Control*. Springer, Berlin, Heidelberg, 2005, pp. 3–22.
- [22] B. Houska, H. J. Ferreau, and M. Diehl, "ACADO toolkit-An open-source framework for automatic control and dynamic optimization," *Optim. Control Appl. Methods*, vol. 32, no. 3, pp. 298–312, 2011.
- [23] R. Tedrake, I. R. Manchester, M. Tobenkin, and J. W. Roberts, "LQR-trees: Feedback Motion Planning via Sums-of-Squares Verification," *Int. J. Rob. Res.*, vol. 29, no. 8, pp. 1038–1052, 2010.
- [24] J. Lofberg, "Pre- and Post-Processing Sum-of-Squares Programs in Practice," *IEEE Trans. Automat. Contr.*, vol. 54, no. 5, pp. 1007–1011, 2009.